

A Data-Driven Bias-Correction-Method-Based Lithium-Ion Battery Modeling Approach for Electric Vehicle Applications

Xianzhi Gong, *Student Member, IEEE*, Rui Xiong, *Member, IEEE*, and Chunting Chris Mi, *Fellow, IEEE*

Abstract—Due to the inconsistent and varied characteristics of lithium-ion battery (LiB) cells, battery pack modeling remains a challenging problem. To model the operation of each cell in the battery pack, considerable work effort and computation time are needed. This paper proposes a data-driven bias-correction-based LiB modeling method, which can significantly reduce the computation work and remain good model accuracy.

Index Terms—Batteries, equivalent circuits, parameter estimation, state estimation, vehicles.

I. INTRODUCTION

DUE to the growing demand of renewal energy and environmental requirements, the lithium-ion battery (LiB) is considered as the major energy storage solution for electric and plug-in hybrid electric vehicles (EVs) due to the high energy and power density characteristics [1]. To manage and maximize the usage of the LiB within the safety margin, the modeling work is essential.

Various state observers such as the Luenberger observer, PI observer, and Kalman filter-based observer have been used in the model-based battery management system (BMS) to estimate immeasurable states such as state of charge (SoC) and state of health (SoH) [2], [12], [14], as shown in Fig. 1. Although these closed-loop feedback-based observers can reduce estimation errors, the structure and accuracy of the LiB model still play a major role in the LiB state estimation.

Manuscript received July 17, 2014; revised January 20, 2015, May 6, 2015, and August 24, 2015; accepted October 1, 2015. Date of publication October 16, 2015; date of current version March 17, 2016. Paper 2014-TSC-0556.R3, presented at the 2014 IEEE Transportation Electrification Conference and Expo, Dearborn, MI, USA, June 15–18, and approved for publication in the IEEE TRANSACTIONS ON INDUSTRY APPLICATIONS by the Transportation Systems Committee of the IEEE Industry Applications Society. This work was supported in part by the U.S. Department of Energy (DOE) under Grant DEEE0002720 and Grant DE-EE0005565, in part by the U.S. DOE Graduate Automotive Technology Education Grant, and in part by the National Natural Science Foundation of China under Grant 51507012.

X. Gong is with the Department of Electrical and Computer Engineering, University of Michigan–Dearborn, Dearborn, MI 48128 USA.

R. Xiong is with the National Engineering Laboratory for Electric Vehicles, School of Mechanical Engineering, Beijing Institute of Technology, Beijing 100081, China.

C. C. Mi is with the Department of Electrical and Computer Engineering, San Diego State University, San Diego, CA 92130 USA (e-mail: mi@ieee.org).

Color versions of one or more of the figures in this paper are available online at <http://ieeexplore.ieee.org>.

Digital Object Identifier 10.1109/TIA.2015.2491889

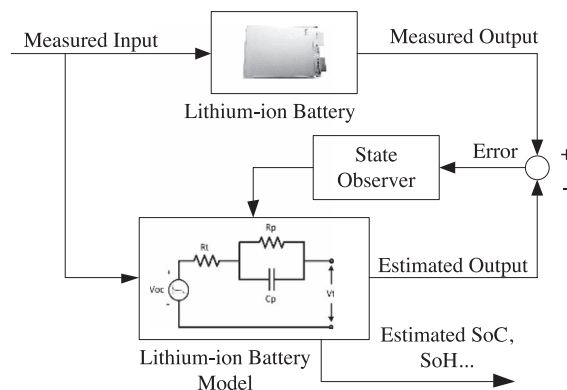


Fig. 1. Diagram of a typical model-based LiB state estimation system.

Due to the initial inconsistency and various aging levels, the characteristics of each cell in the battery pack, such as open-circuit voltage (OCV), polarization effects, and internal resistance, can be different [3], [4], [14]. Conventional equivalent circuit-based modeling methods such as [15]–[17] have to identify the model parameters through individual tests such as hybrid pulse power characterization (HPPC) test, which is highly impractical and time consuming in actual EV application. Building the model of a battery pack composed of hundreds of cells in series and parallel requires a significant amount of work effort and time.

In this paper, we propose a data-driven model bias-correction method based on increment capacity analysis (ICA), which can quickly identify the lumped model of LiB packs during the battery charging process. The inconsistency characteristics of LiB cells with different aging levels will be discussed based on the test results of a LiB pack from a used pickup truck EV. Model bias-correction functions of cells will be derived from the ICA test. Then, the model of each individual cell can be obtained from the standard reference cell model with bias-correction functions. Finally, the lumped LiB pack model can be built by these individual cell models online. Experimental results demonstrate that the model accuracy with this bias-correction method is satisfactory and the modeling work effort can be significantly reduced.

II. BATTERY MODEL AND PARAMETER IDENTIFICATION

A. Basis of Battery Modeling

The electrical behavior of a LiB can be regarded as the behavior of a combination of voltage source with passive elements

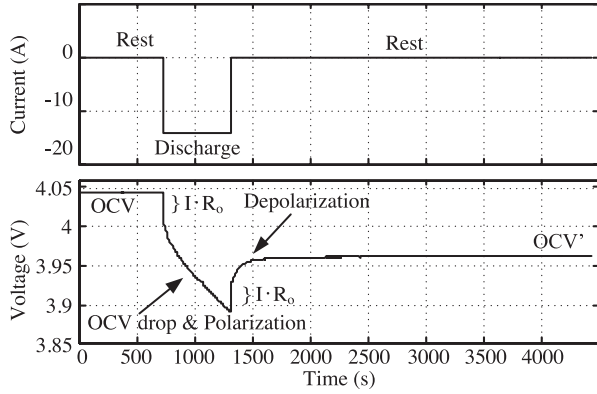


Fig. 2. Typical LiB terminal voltage response at discharging and rest. (Top) Current. (Bottom) Terminal voltage.

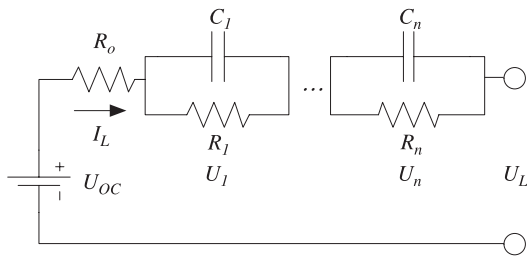


Fig. 3. RC network-based equivalent circuit LiB model.

such as resistors and capacitors [5]. It is noted that the voltage source and passive elements are usually multiple factors dependent rather than constants. For example, the voltage source, which represents the OCV, is a function of SoC, SoH, and temperature.

The SoC, as one of the most important states in LiB, indicates how much energy can be extracted from the LiB and is also an internal state that cannot be measured directly. The conventional SoC estimation method is based on current integration, which is an open-loop method and can be easily influenced by cumulative noise. As shown in Fig. 1, the model-based SoC estimation method is a closed-loop method that can resist the noise from the operation environment and provide better performance. It uses the correlation between SoC and OCV to examine and correct the SoC estimation result. To obtain the OCV, the conventional method is to fully relax the LiB after discharging or charging, which is not practical during the EV operation. Therefore, the OCV used in the BMS for SoC estimation is calculated from the LiB model.

The typical voltage response of a LiB at discharging is shown in Fig. 2. Once the LiB is being discharged, the terminal voltage instantly drops due to the ohmic resistance R_o . Then, the terminal voltage keeps decreasing due to the OCV drop and polarization effect. Once discharging is finished, the terminal voltage instantly increases and then slowly returns to a new OCV (OCV') through the depolarization process. Intuitively, dynamic behavior of LiB can be modeled by the RC network-based lumped parameter equivalent circuit model in Fig. 3 [6].

In this model, U_{oc} represents the OCV; R_o represents the ohmic resistance; and C_n and R_n form the RC networks that

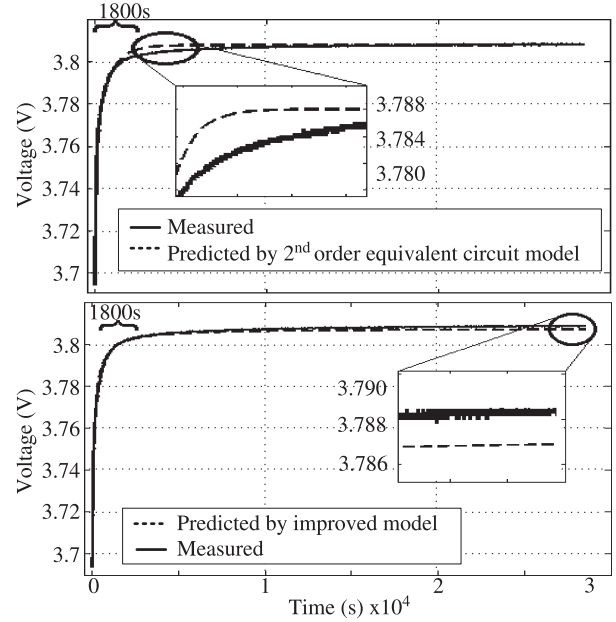


Fig. 4. Typical LiB terminal voltage response at discharging and rest. (Top) Current. (Bottom) Terminal voltage.

represent the dynamic behaviors of the LiB, i.e., the polarization and depolarization processes. The transfer function of this model can be written as

$$U_L(s) = U_{oc}(s) - I_L(s) \times \left(R_o + \frac{R_1}{1 + R_1 C_1 s} + \dots + \frac{R_n}{1 + R_n C_n s} \right) \quad (1)$$

$$\tau_n = R_n C_n \quad (2)$$

where τ is the time constant of the RC network, I_L is the load current, and U_L is the LiB terminal voltage.

From [4], the recurrence equation of the above model can be rewritten as an n -order autoregressive model, as shown in (3). The target vector (4) is built and solved to identify the parameters

$$\varphi_n(k) = [1 \quad U_L(k-1) \dots U_L(k-n) \quad I_L(k-1) \dots I_L(k-n)] \quad (3)$$

$$\theta_n(k) = \left[\left(1 - \sum_{i=1}^n c_i \right) U_{oc}(k) \quad c_1 \quad \dots \quad c_{2n+1} \right]^T \quad (4)$$

B. Improved LiB Model With OCV Prediction

The model accuracy of RC network-based equivalent circuit battery mainly depends on the RC networks' order and the length of fitting data. Therefore, the OCV prediction error produced by using the RC networks model usually increases over time. As shown in the top part of Fig. 4, the estimation result of the second-order RC network-based LiB model is still insufficient when the fitting data length is 1800 s.

In [7], an OCV prediction method was proposed that uses a time-varying time constant instead of the fixed time constant used in the RC network-based model. The time-varying time

constant can be identified online. The improved model can be described by using the following simple first-order linear functions

$$U_L(t) = OCV - C_0 \cdot \exp\left(\frac{t}{\tau(t)}\right) - i \cdot R_o \quad (6)$$

$$\tau(t) = \alpha \cdot t + \beta \quad (7)$$

where C_0 is the polarization coefficient and α, β are the time-varying parameters. The second-order RC network model is reduced to one-order RC network based with a time-varying time constant, which reduces the computational complexity and identification work effort significantly. The bottom part of Fig. 4 shows that the maximum error of the prediction is within 3 mV after 8 h relaxation by applying the first 1800 s' terminal voltages data.

III. DATA-DRIVEN MODEL BIAS-CORRECTION METHOD

One common problem in LiB pack modeling is the inconsistent and varied characteristics of individual LiB cells [8]. These inconsistencies are mainly reflected in the performance uncertainty, even if all these LiB cells, are the same type and from the same manufacturer. On the one hand, uncertainties during the manufacturing process, such as impurities in electrode and electrolyte material, may cause the initial inconsistency. On the other hand, the inconsistency is also related to the different aging effects of LiB cells caused by different operation profiles and environment, such as the temperature, C-rate, and depth of discharge [6]. For the LiB pack modeling, one solution is to identify each cell in the pack individually, which is very time-consuming and inefficient. To improve the suitability of the LiB model for cells with different characteristics and aging levels, we developed a data-driven model bias-correction method to simplify the modeling process and remain good accuracy.

This brief procedure of the proposed bias-correction method can be summarized as follows: First, a standard fresh LiB cell from the pack is selected as the reference cell. The ICA and HPPC tests are applied to this cell to build the reference model and reference dQ/dV curve. Then, we select several cells with different aging levels to identify the characteristics' differences and dQ/dV curves either. Based on acquired data and correlation analysis between these difference and dQ/dV curves, the bias-correction functions can be built. Finally, individual LiB cell can be modeled based on the reference cell model and associated bias-correction functions, which only requires the CC charging voltage data.

Compared with the HPPC modeling method, one advantage of this method is that it only needs the voltage data during the battery constant current charging stage. Therefore, model of each cell in the series-connected pack, which shares same current, can be updated online during the daily battery charging process, as shown in Fig. 5. These updated cell models can form the lumped pack model to track the aging effect of LiB pack and provide better state estimation results in the BMS.

A. Analysis of the Inconsistency Characteristics of a LiB

A LiB pack that is composed of 50 cells is selected as the experimental subject, as shown in Fig. 6. This LiB pack

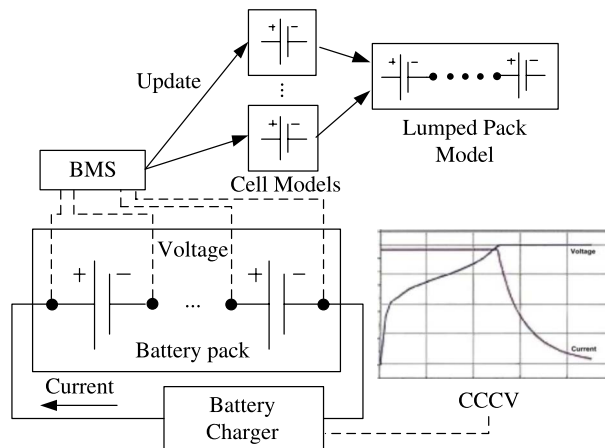


Fig. 5. Overview of the lumped LiB pack model updating through the CCCV charging process.



Fig. 6. Used LiB pack composed of 50 cells in series.

TABLE I
DATASHEET OF TESTED LiB

Positive electrode	Nickel-Cobalt-Manganese-Oxide
Negative electrode	Graphite
Nominal voltage	3.7 V
Upper limit voltage	4.05 V
Lower limit voltage	3V
Nominal capacity	32 Ah
Cell #1 capacity	22.13 Ah
Cell #2 capacity	31.87 Ah
Cell #3 capacity	24.25 Ah

is disassembled from a prototype pickup EV that has been operated in real road testing for three years. The datasheet of the LiB is shown in Table I.

These 50 cells are connected in series to form a pack, which means that they share the same charge/discharge currents. However, the aging levels of cells are different. The capacity statistic result of these 50 cells measured at 0.5 C-rate is shown in Fig. 6. The average capacity of all cells is 28.25 Ah; the maximum capacity is 35.52 Ah, and the minimum capacity is 19.17 Ah. The histogram (see Fig. 7) indicates that the capacities of the 50 cells roughly follow the Gaussian distribution. Three cells from the LiB pack, including two cells (Cells #1 and #3)

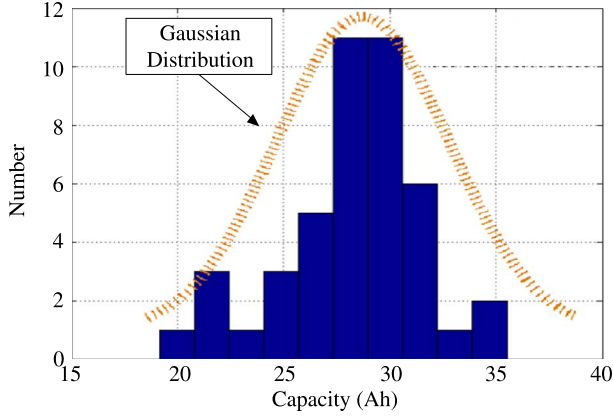


Fig. 7. Histogram of 50 LiB cells' capacities. Average: 28.25 Ah. Maximum: 35.52 Ah. Minimum: 19.17 Ah.

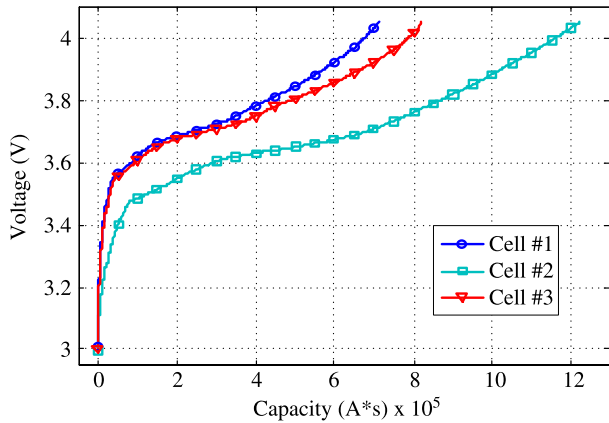


Fig. 8. OCV curves of Cells #1-3 as functions of capacities.

with similar aging levels and one fresher cell (Cell #2), are selected as the experimental examples to demonstrate the modeling procedure of the proposed bias-correction method in the following context.

In general, the inconsistency of LiB characteristics can be divided into the following aspects [9].

1) *OCV Inconsistency*: As one of the most important parts in the LiB model, the OCV represents the LiB potential, which is determined by the Li-ion concentration on the surface of active material particles. The OCV curves can be acquired through low-current (1/30 C) charge/discharge tests or long depolarization rest (> 3 h) tests at different SoCs spanning the entire range.

The OCV curves of Cells #1-3 as functions of capacities and normalized SoC are shown in Figs. 8 and 9. For Cells #1 and #3, which have similar aging level, the normalized OCV curves appear to overlap. On the contrary, the OCV difference between Cell #2 and Cells #1 and 3 is significant, where the maximum difference is 10 mV at around 20% SoC.

2) *Ohmic Resistance and Polarization RC Network Time Constant Inconsistency*: The ohmic resistance R_o and RC network time constant τ in the LiB model are used to represent the dynamic behavior of LiBs. Typically, HPPC tests are used to acquire the current and voltage data to identify these parameters.

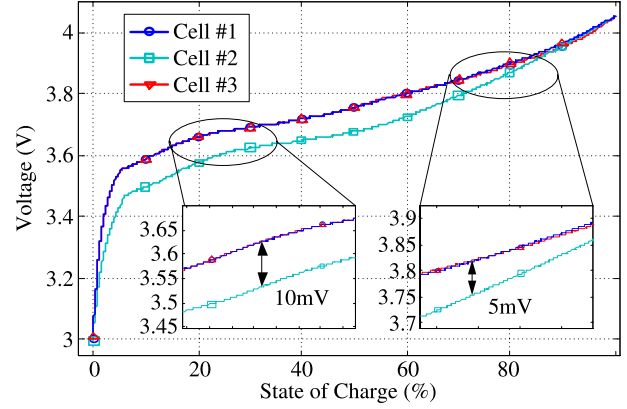


Fig. 9. Normalized OCV curves of Cells #1-3 as functions of SoC.

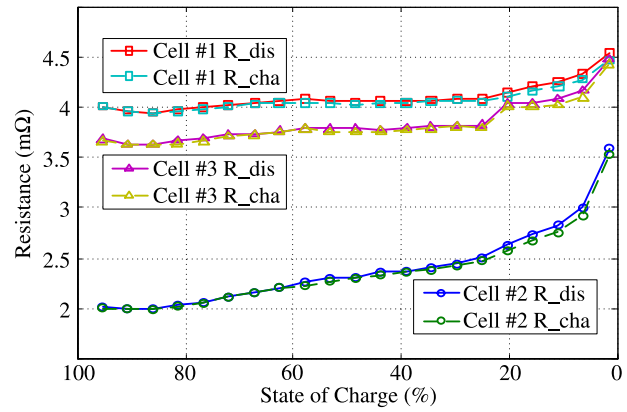


Fig. 10. Ohmic resistance of Cells #1-3 at various SoCs.

The ohmic resistances R_o of the three cells are plotted in Fig. 10, where R_{cha} and R_{dis} denote the ohmic resistance in the charging and discharging processes, respectively. It is found that R_o is a function of the SoC and independent of the load current. The highest ohmic resistance appears at the end of SoC.

The RC network time constants in LiB models are used to represent the polarization and depolarization processes in LiBs during charging/discharging and the rest stage. Time constants are nonlinear functions of SoC, wherein the relationship between the time constant and SoC is hard to describe precisely. However, in most cases, the time constant is longer when SoC is low, which means that the polarization effect is more severe.

B. Bias-Correction Method Based on ICA

From the previous sections, the inconsistency in the LiB cells with different aging levels can be summarized as the difference of capacities, OCVs, ohmic resistances, and polarization processes. Once these differences are identified, models of each cell in the LiB pack can be established in the base of the reference LiB model and bias functions, as shown in Fig. 11.

To obtain and analyze these differences in the LiB, a powerful tool called ICA has been used. The core of the ICA method is based on the dQ/dV curve, where Q is denoted as capacity and V is the terminal voltage. The ICA method converts the plateau phenomenon of LiB into peaks in the dQ/dV curves, which can express the lithium intercalation process and staging phenomenon clearly [10], [11].

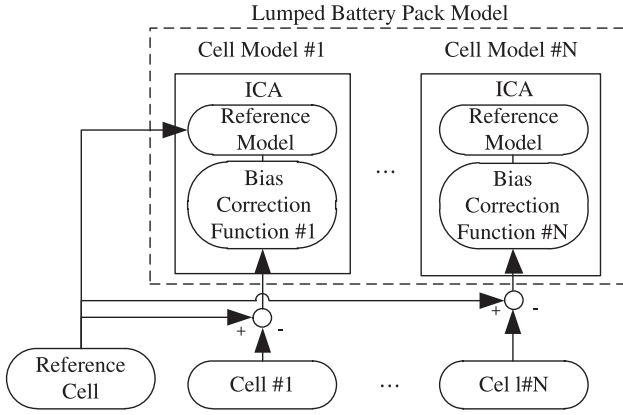
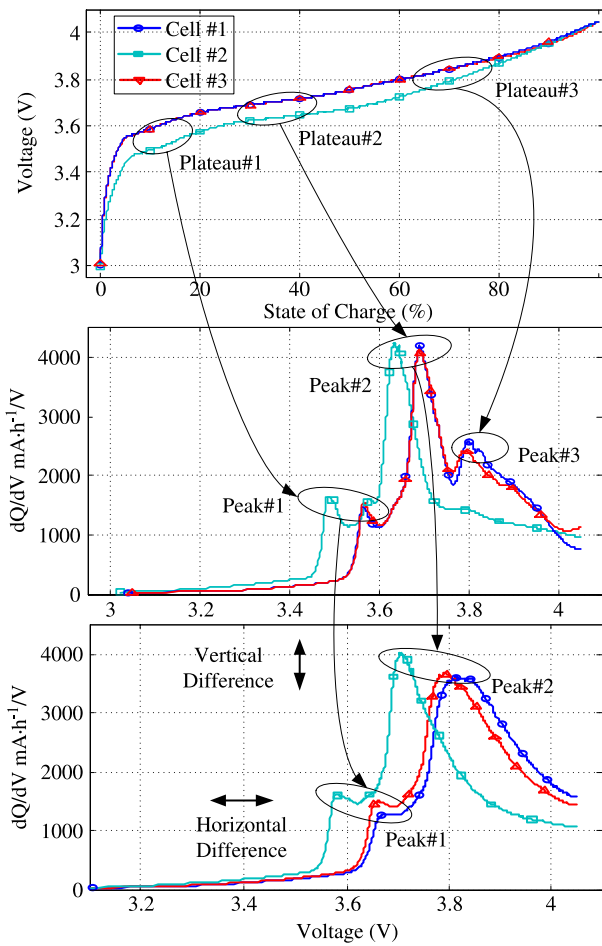


Fig. 11. ICA-based bias function modeling flowchart.

Fig. 12. CC charging voltage curves and ICA test results of Cells #1, 2, and 3. (Top) 1/30 C-rate charging voltage. (Middle) 1/30 C-rate dQ/dV . (Bottom) 1/2 C-rate dQ/dV .

The ICA test results of Cells #1–3 at different current rates are shown in Fig. 12. The dQ/dV peaks shown in the vertical axis indicate that plateau phenomenon occurs in the corresponding LiB voltage range. Typically, the plateau phenomenon is related to the LiB electrodes' active material phase change processes, which can be used to evaluate the aging level [11]. Compared with the ICA result at normal current rate (1/2 C) charging in the bottom part, the ICA result at low current rate charging (1/30 C) in the top part shows more detailed

information on the three main dQ/dV changing peaks #1–3, located in the voltage range of 3.5–3.8 V, which denote three plateau phenomena at the CC voltage curve. However, the ohmic resistance differences between these three cells are hard to identify due to the low current. In practice, the typical charging current of EVs is from 1/8 C (SAE J1772 ac Level-I household charger) to 2 C rate (SAE J1772 dc Level-II high-power dc charge station). In other words, the charging time is from 8 h to 30 min, which means that the low-current ICA test is not suitable for EV applications. Considering the practical feasibility together with the tradeoff between accuracy and work effort, the normal charging current rate (1/2 C) is applied in the ICA tests to build the bias-correction functions.

Since the main plateau phenomenon always happens at the same OCV range in LiBs with the same electrode active material, the horizontal differences in dQ/dV peak #2 can be used to represent the ohmic resistance inconsistency. Setting the identification results from the HPPC test as the reference, the goodness of estimation results based on the ICA method is up to 87%, which shows that the ICA test results can identify the ohmic resistance very well. The vertical and horizontal differences of both peaks #1 and #2 are used jointly to represent the capacity and OCV differences. Based on the ICA test results, the improved model with bias-correction functions $f_n(ICA_n, ICA_0)$ can be written as

$$\begin{cases} R'_o(\text{SoC}) = R_o(\text{SoC}) + f_1(ICA_n, ICA_0, \text{SoC}) \\ \alpha'(\text{SoC}) = \alpha(\text{SoC}) + f_2(ICA_n, ICA_0, \text{SoC}) \\ \beta'(\text{SoC}) = \beta(\text{SoC}) + f_3(ICA_n, ICA_0, \text{SoC}) \\ \text{OCV}'(\text{SoC}) = \text{OCV}(\text{SoC}) + f_4(ICA_n, ICA_0, \text{SoC}) \end{cases} \quad (8)$$

where ICA_0 and ICA_n denote the reference and target LiB cells' ICA test result curves, respectively; R_o , α , β and R'_o , α' , β' denote the ohmic resistance and model parameters of the reference and target LiB cells. The curve fitting-based empirical method is used to obtain the bias-correction functions $f_n(ICA_n, ICA_0, \text{SoC})$ as follows:

$$\begin{cases} f_1 = (23 \times (V_n - V_0)^2 + 17 \times (V_n - V_0)) * 10^{-2} \times f(\text{SoC}) \\ \text{when } \left(V \in \left(dQ/dV > \max \left(\frac{dQ}{dV} \right) \right) \right) \\ f(\text{SoC}) = 0.507 + 0.0107 \times \text{SoC} - 0.000587 \times \text{SoC}^2 \end{cases} \quad (9)$$

$$\begin{cases} f_2 = \frac{\int_{3.5}^4 (dQ/dV_n - dQ/dV_0) dV}{4 - 3.5} \times 0.27 \\ f_3 = 0 \end{cases} \quad (10)$$

$$\begin{cases} f_4 = (0.03 \times (V_n - V_0)^2 + (V_n - V_0)) \times f(\text{SoC}) \\ \text{when } \left(V \in \left(\frac{d(dQ/dV)}{dV} < 0 \right) \right) \\ f(\text{SoC}) = 0.418 + 0.0353 \times \text{SoC} - 3.83 \times 10^{-3} \times \text{SoC}^2 \end{cases} \quad (11)$$

where V_0 denotes the horizontal axis position, i.e., the voltage of the reference ICA test peak #2 result, whereas V_n denotes the voltage of the target ICA test peak #2 result. In function f_1 (9), the ohmic resistance difference is represented by the lateral displacement of voltage together with the second-order SoC

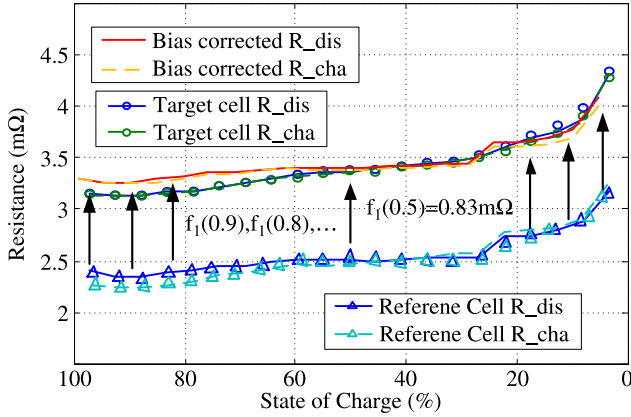


Fig. 13. Ohmic resistance calculation example. Measured target cell ohmic resistance and the calculated bias-corrected ohmic resistance based on the reference model.

TABLE II
CORRECTED OHMIC RESISTANCE AND MEASURED VALUE

SoC (%)	Corrected resistance (mΩ)	Measured resistance (mΩ)
100	3.35	3.27
50	3.4	3.39
10	3.78	3.81

polynomial function, where the lateral displacement voltage should be higher than maximum dQ/dV point than (peak #2). For relaxation processes, a simple average peak voltage-based empirical function (10) is applied. Finally, the OCV bias function is based on the horizontal voltage shift when the derivative of dQ/dV curve is lower than zero.

The modeling result of cell #1 as the target cell and cell #2 as the reference cell is shown in Fig. 13 and Table II as an example. In this example, the horizontal voltage difference of the main ICA peaks #2 and #1 between the target cell and the reference cell is 188 mV (3.889–3.701 V) and 84 mV (3.64–3.556 V); the vertical dQ/dV difference is 384 mA · h⁻¹/V (4011–3627) and 296 mA · h⁻¹/V (1637–1341). The calculation procedure of the 50% SoC case is given below. The bias-corrected and measured ohmic resistances are shown in Table II

$$\begin{cases} f_1 = (23 \times (3.889 - 3.701)^2 + 17 \times (3.889 - 3.701) \\ \quad \times 10^{-2} \times f(0.5) \quad \text{when } (V \in (dQ/dV > \max(\frac{dQ}{dV}))) \\ f(0.5) = 0.507 + 0.0107 \times 0.5 - 0.000587 \times 0.5^2 = 0.512 \\ f_1 = 23 \times 0.188^2 + 17 \times 0.188 \times 10^{-2} \times 0.512 = 0.82927 \text{ m}\Omega \\ f_2 = \frac{\int_{3.5}^4 (dQ/dV_n - dQ/dV_0) dV}{4 - 3.5} \times 0.27 = 0.82927 \text{ m}\Omega \\ \begin{cases} f_4 = (0.03 \times (V_n - V_0)^2 + (V_n - V_0)) \times f(0.5) \\ \quad \text{when } (V \in (dQ/dV > \text{inflection point}(\frac{dQ}{dV}))) \\ f(0.5) = 0.418 + 0.0353 \times 0.5 - 3.83 \times 10^{-3} \times 0.5^2 = 0.436 \\ f_4 = (0.03 \times 0.227^2 + 0.227) \times 0.436 = 0.0996 \text{ V.} \end{cases} \end{cases}$$

IV. VERIFICATION AND DISCUSSION

To evaluate the bias-correction method, the federal urban driving schedule (FUDS) is applied to all 50 LiB cells by using

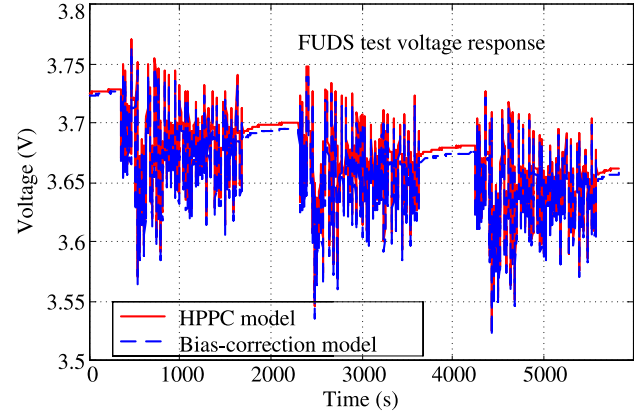


Fig. 14. Model's output of Cell #1 under FUDS tests. (Blue) Model based on bias-correction method. (Red) Model based on HPPC tests.

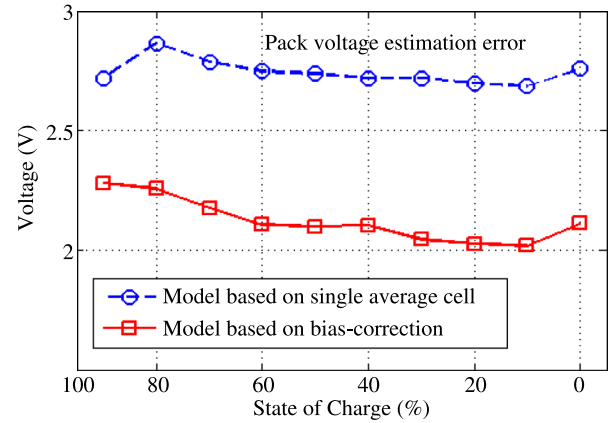


Fig. 15. Model output error comparison of 50-cell LiB pack. (Blue) Single-average-cell-based model. (Red) Proposed bias-correction method.

the Arbin BT2000 battery cycler. The fresh LiB cell is selected as a benchmark to build the reference model. Compared with the standard HPPC method, the voltage prediction result remains good, and the average voltage differences of all 50 LiB cells are within 12 mV. The voltage prediction results of Cell #1 by using both the bias-correction method and the conventional HPPC modeling method are displayed in Fig. 14.

Then, the 50-cell LiB pack lumped model are built by adding all 50 bias-corrected individual cell models together. As shown in Fig. 15, the voltage prediction error comparison of the proposed bias-correction method (2.25 V for 50 cells) and the uncorrected single-cell method (3.03 V for 50 cells) shows that the error of the proposed modeling method is much lower. It is noted that the prediction error of each cell is less than 45 mV (2.25 V/50 cells), which is close to the standard HPPC method (25–35 mV). However, the model error slightly increases when SoC reaches 85% and higher. This is because the dQ/dV peak #3 in the high voltage range (3.8–4.05 V) is missed in the ICA tests due to the high charging current (1/2 C). We also expect to improve the estimation accuracy through involving SoC as a state variable in the empirical functions f_2 and f_3 through further study and investigation of the correlation between the temperature, aging level, polarization effect, and ICA test.

V. CONCLUSION

A data-driven bias-correction method-based LiB modeling approach for EV application has been proposed in this paper. The basics of equivalent circuit LiB models and techniques to improve terminal voltage prediction are discussed. A modified one-order *RC* network-based LiB model can sufficiently simulate the dynamic voltage behavior using a simplified structure.

Multiple aspects of the inconsistency of LiBs are studied through the experimental test results of a 50-cell LiB pack from a used pickup EV. The results indicate that the inconsistency of LiB characteristics can be summarized as the OCV inconsistency, ohmic resistance inconsistency, and the dynamic behavior inconsistency. Based on the above analysis, a bias-correction modeling method is proposed. This bias-correction method uses the difference of ICA test results between the target cell and the reference cell to build the LiB models, which only requires simple voltage data during constant current charging. An example of ohmic resistance bias-correction procedure is also demonstrated.

Finally, the lumped model of 50-cell LiB pack is built based on the proposed bias function method. The simulation results show that the prediction error is within 2.25 V for the entire pack or an average of 45 mV for each cell. Compared with the lumped pack model based on a single average cell, the accuracy of the pack model based on the proposed bias-correction method remains good, whereas the modeling work effort is significantly simplified.

REFERENCES

- [1] C. C. Mi, A. Masrur, and W. Gao, *Modern Hybrid Electric Vehicles*. New York, NY, USA: Wiley, 2011.
- [2] J. Xu *et al.*, "State of charge estimation of lithium-ion batteries based on the proportional integral observers," *IEEE Trans. Veh. Technol.*, vol. 63, no. 4, pp. 1614–1621, May 2014.
- [3] J. Shen, S. Dusmez, and A. Khaligh, "An advanced electro-thermal cycle-lifetime estimation model for LiFePO₄ batteries," in *Proc. ITEC*, 2013, pp. 1–6.
- [4] R. Xiong, F. Sun, X. Gong, and H. He, "Adaptive state of charge estimator for lithium-ion cells series battery pack in electric vehicles," *J. Power Sources*, vol. 242, pp. 699–713, Nov. 2013.
- [5] H. He, R. Xiong, X. Zhang, and F. Sun, "State-of-charge estimation of the lithium-ion battery using an adaptive extended Kalman filter based on an improved Thevenin model," *IEEE Trans. Veh. Technol.*, vol. 60, no. 4, pp. 1461–1469, May 2011.
- [6] X. Gong, R. Xiong, and C. C. Mi, "Study of the characteristics of battery packs in electric vehicles with parallel-connected lithium-ion battery cells," *IEEE Trans. Ind. Appl.*, vol. 51, no. 2, pp. 1872–1879, Mar./Apr. 2015.
- [7] L. Pei, T. Wang, R. Lu, and C. Zhu, "Development of a voltage relaxation model for rapid open-circuit voltage prediction in lithium-ion batteries," *J. Power Sources*, vol. 253, pp. 412–418, May 2014.
- [8] Z. Xi, R. Jing, and G. Y. Xiao, "State of charge estimation of lithium-ion batteries considering model and parameter uncertainties," in *Proc. Annu. Conf. Prognostics Health Manage. Soc.*, 2013, pp. 1–8.
- [9] B. Y. Liaw, R. G. Jungst, G. Nagasubramanian, H. L. Case, and D. H. Doughty, "Modeling capacity fade in lithium-ion cells," *J. Power Sources*, vol. 140, no. 1, pp. 157–161, Jan. 2005.
- [10] C. Weng, Y. Cui, S. Jing, and H. Peng, "On-board state of health monitoring of lithium-ion batteries using incremental capacity analysis with support vector regression," *J. Power Sources*, vol. 235, pp. 36–44, Aug. 2013.
- [11] M. Dubarry, V. Svoboda, R. Hwu, and B. Y. Liaw, "Incremental capacity analysis and close-to-equilibrium OCV measurements to quantify capacity fade in commercial rechargeable lithium batteries," *Electrochem. Solid State Lett.*, vol. 9, no. 10, p. A454, 2006.
- [12] C. Hu, B. D. Youn, and J. Chung, "A multiscale framework with extended Kalman filter for lithium-ion battery SOC and capacity estimation," *Appl. Energy*, vol. 92, pp. 694–704, Apr. 2012.
- [13] Y. Xing, W. He, M. Pecht, and K. L. Tsui, "State of charge estimation of lithium-ion batteries using the open-circuit voltage at various ambient temperatures," *Appl. Energy*, vol. 113, pp. 106–115, Jan. 2014.
- [14] W. He, N. Williard, M. Osterman, and M. Pecht, "Prognostics of lithium-ion batteries based on Dempster–Shafer theory and the Bayesian Monte Carlo method," *J. Power Sources*, vol. 196, pp. 10314–10321, 2011.
- [15] Y. Hu and S. Yurkovich, "Battery cell state-of-charge estimation using linear parameter varying system techniques," *J. Power Sources*, vol. 198, pp. 338–350, Jan. 2012.
- [16] G. L. Plett, "Extended Kalman filtering for battery management systems of LiPB based HEV battery packs," *J. Power Sources*, vol. 134, no. 2, pp. 277–92, Aug. 2004.
- [17] R. Xiong, H. He, F. Sun, X. Liu, and Z. Liu, "Model-based state of charge and peak power capability joint estimation of lithium-ion battery in plug-in hybrid electric vehicles," *J. Power Sources*, vol. 229, pp. 159–169, May 2012.



Xianzhi Gong (S'10) received the B.S. degree in electrical engineering and automation from Nanjing University of Aeronautics and Astronautics, Nanjing, China, in 2009 and the M.S. degree in electrical engineering from the University of New Haven, West Haven, CT, USA, in 2011. He is currently working toward the Ph.D. degree in automotive systems engineering in the Graduate Automotive Technology Education Center for Electric Drive Transportation, University of Michigan–Dearborn, Dearborn, MI, USA.

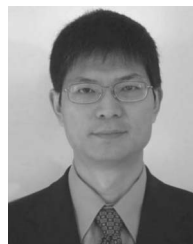
His research interests include battery management, power electronics for electric vehicles, and renewable energy.



Rui Xiong (S'12–M'14) received the M.Sc. degree in vehicle engineering and the Ph.D. degree in mechanical engineering from Beijing Institute of Technology, Beijing, China, in 2010 and 2014, respectively. From 2012 to 2014, he was a joint Ph.D. student with the U.S. Department of Energy Graduate Automotive Technology Education Center for Electric Drive Transportation, University of Michigan–Dearborn, Dearborn, MI, USA.

Since 2014, he has been an Associate Professor with the Department of Vehicle Engineering, School of Mechanical Engineering, Beijing Institute of Technology. During 2015, he was a Visiting Associate Professor with the Faculty of Science, Engineering and Technology, Swinburne University of Technology, Hawthorn, Australia. His research focuses mainly on electrical/hybrid vehicles, energy storage systems, and battery management systems.

Dr. Xiong was a recipient of the Excellent Doctoral Dissertation Award from Beijing Institute of Technology in 2014. He received Best Paper Awards from the journal *Energies* and the National 100 Most Influential International Academic Papers from the Institute of Scientific and Technical Information of China in 2015 and 2014, respectively.



Chunting Chris Mi (S'00–A'01–M'01–SM'03–F'12) received the B.S.E.E. and M.S.E.E. degrees from Northwestern Polytechnical University, Xi'an, China, in 1981 and 1988, respectively, and the Ph.D. degree from the University of Toronto, Toronto, ON, Canada, in 2001, all in electrical engineering.

He is currently a Professor and the Chair of the Department of Electrical and Computer Engineering, San Diego State University, San Diego, CA, USA. He was previously with the University of Michigan–Dearborn, Dearborn, MI, USA, from 2001 to 2015.

He has conducted extensive research and has published more than 100 articles. His research interests include electric drives, power electronics, electric machines, renewable energy systems, and electrical and hybrid vehicles.

Dr. Mi is an Associate Editor of the IEEE TRANSACTIONS ON VEHICULAR TECHNOLOGY, IEEE TRANSACTIONS ON POWER ELECTRONICS, and IEEE POWER ELECTRONICS LETTERS; Associate Editor of the IEEE TRANSACTIONS ON INDUSTRY APPLICATIONS; and Senior Editor of the *IEEE Vehicular Technology Magazine*. He is a Guest Editor of the *International Journal of Power Electronics*.